Available online at www.sciencedirect.com
SCIENCE DIRECT
Journal of Nuclear Materials 348 (2006) 70–78
journal of nuclear materials
www.elsevier.com/locate/jnucmat

Crystallization of lanthanum and yttrium aluminosilicate glasses

Najim Sadiki [a,*], Jean Pierre Coutures [a], Catherine Fillet [b], Jean Luc Dussossoy [b]

[a] Procédés, Matériaux et Energie Solaire (PROMES), Rambla de la Thermodynamique, Tecnosud, 66100 Perpignan, France
[b] SCDV/LEBV CEA Valrho Marcoule B.P 17171 30207 Bagnols-Sur-Ceze cedex, France

Received 10 May 2005; accepted 2 September 2005

Abstract

The crystallization behaviour of aluminosilicate glasses of lanthanum (LAS) and yttrium (YAS) containing 2–8 mol% of Ln_2O_3 (Ln = La or Y), 12–30 mol% of Al_2O_3, and 64–80 mol% of SiO_2 has been studied by DTA, XRD and SEM-EDX analysis. X-ray diffraction results indicate the presence of the mullite phase and $La_2Si_2O_7$ in the monoclinic high-temperature G form (group space $P2_1/c$) for the LAS glasses, and mullite y-$Y_2Si_2O_7$ in the monoclinic structure (group space C2/m) and a small amount of β-$Y_2Si_2O_7$ in the orthorhombic structure (space group Pna2) for the YAS. For both cases, very little tridymite phase is observed. The results also show that the values of T_g for YAS are higher than those for LAS glasses. The crystallization of LAS glasses is more difficult than that of YAS. For all samples, we observed only one kind of mullite (Al/Si = 3.14).

1. Introduction

Yttrium and rare earth aluminosilicate glasses have similar and interesting physical properties and previous studies of the vitreous phases in the Ln_2O–Al_2O_3–SiO_2 (Ln = La → Lu and Y) have shown that the glassy zone decreases with the ionic field strength (z/r^2) of the Ln^{3+} cation [1–7] (z: Ln valency, r ionic radii). These glasses have high glass-transition temperatures [1–3,8], interesting mechanical properties such as high hardness and elastic modulus [4,5,9,10], and a great chemical durability [11–13]. These glasses have a large range of applications in modern technology, for example, as a host material in laser applications, for bonding of silicon nitride ceramics, and a matrix for storage of long-lived actinides. Our work is concerned mainly with the application of these glasses as a matrix for the conditioning of long-lived actinides. Lanthanum and yttrium have been chosen to simulate trivalent actinides because firstly their phase diagrams are known as well as relevant physico-chemical properties, and secondly spectroscopic studies with multinuclear (^{27}Al and ^{17}O) NMR can be carried out to obtain structural information without the problems of paramagnetism presented by the other lanthanide cations.

However, it is important to point out the discrepancies observed in the reported phase diagrams of

* Corresponding author. Tel.: +33 4 68 68 22 48; fax: +33 4 68 68 22 13.
E-mail address: sadiki@univ-perp.fr (N. Sadiki).

0022-3115/$ - see front matter © 2005 Elsevier B.V. All rights reserved.
doi:10.1016/j.jnucmat.2005.09.003

the constituent binary subsystems such as Ln_2O_3–Al_2O_3, Ln_2O_3–SiO_2 and Al_2O_3–SiO_2. For example, a critical assessment of only Ln_2O_3–Al_2O_3 systems has been made by Wu and Pelton [14] using the technique of coupled thermodynamic-phase diagram analysis. For the Ln_2O_3–SiO_2 systems, some thermodynamic modelling has been carried out but essentially of the miscibility gaps and metastability on the rich SiO_2 side [15]. In the last two papers [14,15] references on the experimental phase diagrams could be found. For the two ternary systems, studies of the phase diagram have been respectively carried out on the La_2O_3–Al_2O_3–SiO_2 and Y_2O_3–Al_2O_3–SiO_2 systems by Mazza and Roncheti at 1300 °C in air [16] and by Vomaka and Babushkin [17] up to 1700 °C and under nitrogen. Kolitsch et al. [18] reported the phase relationships in the systems Ln_2O_3–Al_2O_3–SiO2 and recently a thermodynamical assessment of the Y_2O_3–Al_2O_3–SiO_2 system has been given by Fabrichnaya et al. [19] in good agreement with previous experimental work [20,21]. Concerning definite compounds, up to now only one quaternary compound is known with a composition $La_2O_3 \cdot Al_2O_3 \cdot 2SiO_2$ ($LaAlSiO_5$) having an orthorhombic cell and a structure related to tuscanite and latiumite aluminosilicate minerals [18], all of the other definite compounds belonging to the corresponding sub-binaries. For the La_2O_3–Al_2O_3 and Y_2O_3–Al_2O_3 binaries the definite compounds are as follows respectively:

1.1. Aluminate definite compounds with rare earth oxides

Four definite compounds between Al_2O_3 and $(La/Y)_2O_3$ are known to exist namely: (a) The perovskite: $LaAlO_3$ (LA) melting congruently at 2100 °C [22] and having a rhombohedric structure (JCPDS-85-1071) [23], and $YAlO_3$ (YA) with an orthorhombic structure (JCPDS-70-1677) [24] and some discrepancies both in the value of the melting point and its congruent or non-congruent behaviour. (b) Only observed on the binary Y_2O_3–Al_2O_3 phase diagram, the garnet $Y_3Al_5O_{12}$ (3Y5A) with a congruent melting point at 1951 °C [25] and a cubic structure (JCPDS-79-1891) [26] and the monoclinic (JCPDS-34-0368) [27] $Y_4Al_2O_9$ (2YA) compound melting congruently at 2020 °C [28]. The 2LA corresponding compound is known to exist in a moderate temperature range [29]. (c) The β-alumina hexagonal-type structure $LaAl_{11}O_{18}$ (L11A) showing a domain of existence [30] and a non-congruent melting point of 1928 °C.

1.2. Silicate definite compounds with rare earth oxides

A lot of informations concerning the SiO_2–$(La/Y)_2O_3$ definite compounds are available on the literature [31–39] and four compounds are known. The disilicates $La_2Si_2O_7$ (La2S) and $Y_2Si_2O_7$ (Y2S) with a non-congruent melting behaviour at, respectively, 1750 and 1775 °C. La2S is known under two crystallographic forms [31] the tetragonal A form (β-$Ca_2P_2O_7$ structure type) which transforms at 1200 °C into the monoclinic G-form (α-$Ca_2P_2O_7$-type structure). The high temperature G form could be preserved at room temperature during cooling except for slow cooling. Y2S shows a very rich polymorphism, well studied [32–36] with up to possibly six structural forms with the following sequence: z ↔ y (JCPDS- 22-1103) ↔ α (JCPDS-38-0223) ↔ β (JCPDS-82-0732) ↔ γ (JCPDS-45-0042 [37]) ↔ δ (JCPDS-42-0168) occurring respectively at 1030, 1200, 1225, 1445 and 1535 °C. The monosilicates La_2SiO_5 (LS) and Y_2SiO_5(YS) with a congruent melting points respectively at 1930 and 1980 °C, both have a monoclinic structure but with different space groups: LS $P2_1/c$ (JCPDS 40-0234) and YS I2/a (JCPDS-74-2158, [38]). Three other compounds have been reported in these binaries: $La_4Si_3O_{12}$ and $Y_4Si_3O_{12}$ with a congruent melting point respectively at 1975 and 1950 °C, and observable only at high-temperature respectively above 1600 and 1650 °C with a quadratic structure. A third has also been reported with an apatite-like structure of hexagonal symmetry (space group $P6_3/m$) having discrepancies in terms of the right chemical formula and cell parameters [16,39].

The Al_2O_3–SiO_2 phase diagram due to its importance in both earth sciences and modern ceramic technology has been extensively studied with many controversial results [40–43] as far as the liquidus line shape, the melting behaviour of the unique compound the mullite (congruent or non-congruent) and has been reassessed by Erikson and Pelton [44]. Mullite is the only compound of the binary stable under normal T/P conditions. Mullite is a non-stoichiometric compound with the following formula $Al_2^{VI}[Al_{2+2x}Si_{2-2x}]^{IV}O_{10-x}$, $0.17 < x < 0.59$ [45], derived from the well-known sillimanite (Al_2SiO_5) structure, with $x = 0$, obtained by substituting aluminium atoms by silicon in tetrahedral

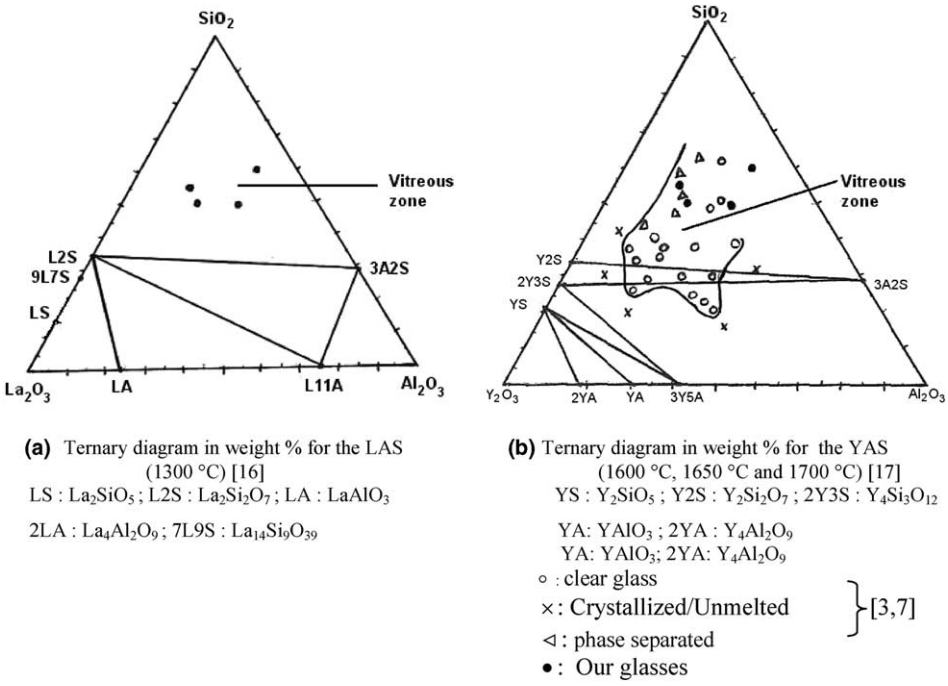

Fig. 1. Schematic representation of the La_2O_3–Al_2O_3–SiO_2 and Y_2O_3–Al_2O_3–SiO_2 ternary systems in weight % with the observed crystalline phases and glass-forming zones.

site, creating oxygen vacancies ($2\ Si^{4+} + O^{2-} \rightarrow 2Al^{3+} + \square$) to preserve the electroneutrality. The solid solution is in $x = 0.17$ to $x = 0.59$ [45] and stoichiometric mullite, $3Al_2O_3$–$2SiO_2$, corresponds to $x = 0.25$. Mullite crystallizes, like the sillimanite, in an orthorhombic structure with the Pbam space group and for the stoichiometric formula the cell parameters are $a = 7.545$ Å, $b = 7.689$ Å, $c = 2.884$ Å (JCPDS 15-776 [46]). The evolution of the cell parameters of the mullite solid solution was firstly shown by Cameron [47] in the eighties and revisited later [43,48]. In Fig. 1, we report schematically the two ternary phase diagrams showing the observed phases and the glass-forming region as known for the YAS system.

2. Experimental

Four compositions (Table 1) were chosen: 10, 20 and 30 wt% of La and Y rare earth oxides, between 50 and 60 wt% in silica in order to meet the requirements of a possible commercialization of these glasses for actinide waste storage. These glasses are called LASn or YASn with $n = 1$–4. All glasses were synthetized starting from the oxides (La_2O_3 99.0% Prolabo, Y_2O_3 99.4% Prolabo, Al_2O_3 99.9%

Table 1
Theoretical and experimental compositions (SEM-EDX) of LAS and YAS glasses

Glass	Starting atomic comp. %				Measured atomic comp. %				Al/Si		Al/(Al+Si)	
	Ln	Al	Si	O	Ln	Al	Si	O	Th.	Exp.	Th.	Exp.
LAS1	4.678	9.97	21.16	64.19	4.78	8.87	21.95	64.39	0.471	0.404	0.320	0.288
LAS2	4.674	7.46	23.22	64.64	4.69	7.45	23.20	64.66	0.321	0.321	0.243	0.243
LAS3	1.35	12.73	21.6	64.32	1.05	12.9	20.52	65.44	0.590	0.628	0.371	0.385
LAS4	2.89	13.76	19.46	63.89	2.94	13.86	20.36	62.85	0.707	0.680	0.414	0.405
YAS1	6.40	9.48	20.11	64.01	6.37	9.49	20.11	64.04	0.470	0.471	0.320	0.320
YAS2	6.37	7.10	22.11	64.42	7.15	7.76	22.20	62.87	0.321	0.349	0.243	0.259
YAS3	1.89	12.55	21.30	64.26	2.54	12.34	22.14	61.75	0.589	0.557	0.370	0.375
YAS4	4.03	13.34	18.86	63.77	4.6	13.24	19.69	64.39	0.707	0.672	0.414	0.402

Pechiney, and SiO_2 Prolabo) carefully mixed and melted under air during around 2 min on a water-cooled aluminium plate associated to a vertical axis laboratory scale solar furnace of 2 kW with an average solar flow (900–1000 W m^{-2}). The cooling rate is around 200 °C s^{-1}, the melting time of two minutes was chosen to satisfied both a good chemical homogeneity of the glasses and no composition shifts due to a preferential vaporization of silica. La_2O_3 was first heat-treated in an alumina crucible during two hours at 1100 °C in order to eliminate anionic impurities and the same heat treatment was applied after the mixing and before melting. After melting, transparent quasi-spherical glassy droplets between 2 and 6 mm in diameter were obtained.

Glass composition was controlled by SEM-EDX analysis after a metallization with gold, the beam energy was 15 keV for glasses and 10 keV for the annealed samples. Glass transition and crystallization temperatures were determined by differential thermal analysis (DTA) with a SETSYS Evolution 1750, SETARAM device. Measurements were done on small glass pieces, placed in a platinum crucible. The reference crucible is an empty platinum crucible. Experiments were carried out up to 1500 °C with a heating rate of 10 °/min. Phase analysis was carried out with an automatic powder diffractometer, Ni filtered CuK_α radiation ($\lambda = 1.54178$ Å) in the 10–70° (2θ) angular range at a scanning speed of 0.4 °/min.

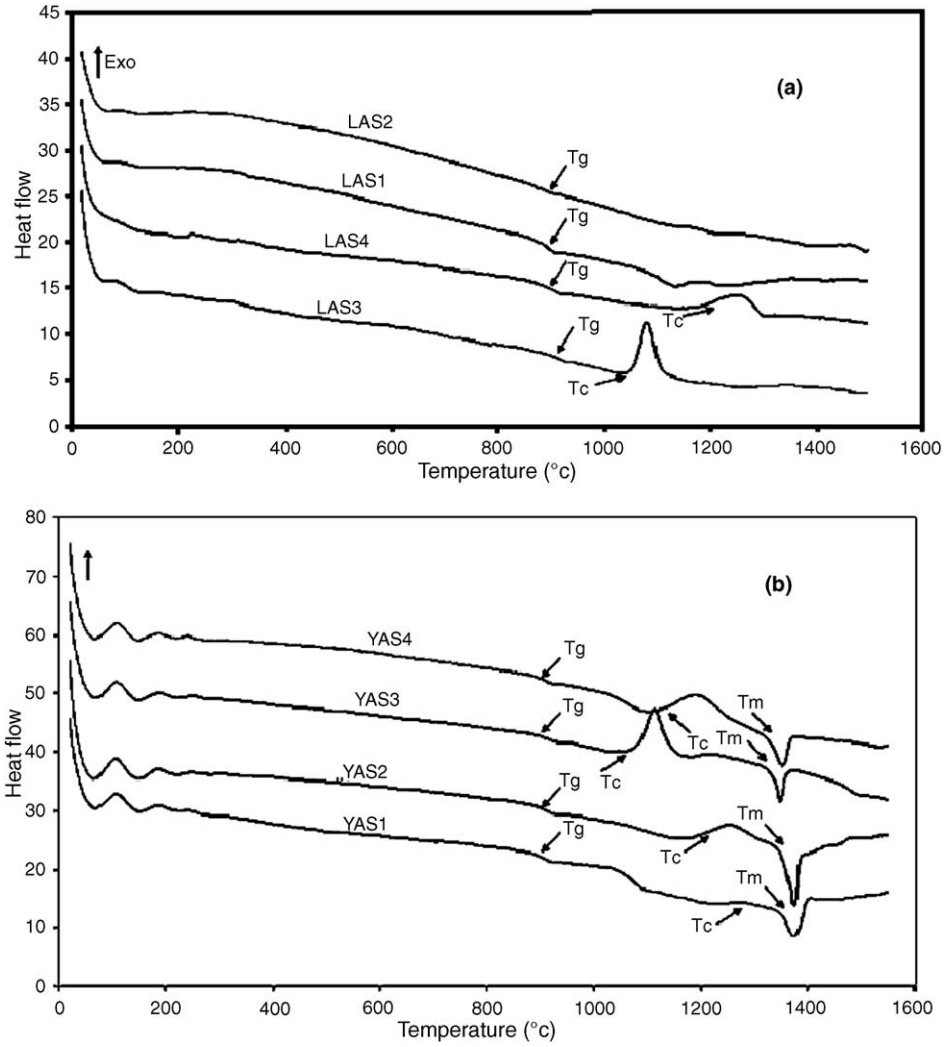

Fig. 2. DTA curves of LAS (a) and YAS (b) glasses (heating rate 10 °C min^{-1}).

3. Results

3.1. Chemical analysis

Glass composition was controlled by SEM-EDX and the results are given in Table 1, each value being an average of about 15 values. We encounter the same problems outlined in the literature concerning the sodium analysis, nevertheless it is clear that the measured Al/Si ratios are in good agreement with the initial theoretical ones.

3.2. Thermal analysis

The results of the DTA analysis of finely crushed LAS and YAS glasses are given in Fig. 2 and Table 2. All curves show a slope change attributed to the glass transition temperature T_g determined to ± 3 °C. Our measured values are in good agreement with previous work [4,8]. Exothermic peaks are due to phases crystallization and endothermic peaks to melting processes. Except for LAS3 and YAS3, crystallization peaks are broad indicating a slow process of crystallization. Endothermic peaks are only observed on YAS glasses and are attributed to a solidus temperature.

3.3. Crystallization

Using the DTA results and to have a better knowledge of the crystallized phases, different annealing processes were carried out at temperature just above the observed crystallization temperature: quite short time annealing (2 h for having good X-ray spectra) and more longer time (5 h up to 15 h) to be more close to equilibrium conditions. The final samples are examined by X-ray diffraction and SEM-EDX. XRD results are given in Table 3 and in Figs. 3–5. All the XRD patterns present a 'vitreous dome' between 20° and 40° in 2θ even for the LAS1 glass annealed for 15 h at 1150 °C reflecting residual glass. The nature of the observed crystallized phases is consistent with the phase diagrams and the results are given in Table 3. In all the XRD spectra where mullite is observed the patterns are of enough good quality to calculate the cell parameters which are reported in Table 3. Using the data of Cameron [47], in particular the curve giving the evolution of a versus the composition in the solid solution range, the composition of the mullite could be obtained. For all the samples, mullite crystallizes with the same composition corresponding to an Al/Si ratio of 3.14 and an x value of the general mullite solid solution formula $Al_2^{VI}[Al_{2+2x}Si_{2-2x}]^{IV}O_{10-x}$ with $x = 0.275$ very close to the value of stoichiometric 3:2 mullite ($x = 0.25$).

To complement the information obtained by XRD, all glasses after the annealing conditions outlined in Table 3 and polishing were examined by SEM. The contrast of the micrographs is better for La than Y glasses and better for the richer La or Y samples. Some examples of the different types

Table 2
Glass transition crystallization and solidus temperatures of LAS and YAS

Glass	Al/Si	T_g (°C)	T_c (°C)	T_{sol} (°C)	Glass	Al/Si	T_g (°C)	T_c (°C)	T_{sol} (°C)
LAS1	0.471	884			YAS1	0.47	913	1220	1358
LAS2	0.321	874			YAS2	0.321	916	1183	1360
LAS3	0.590	910	1055		YAS3	0.589	914	1087	1338
LAS4	0.707	896	1184		YAS4	0.707	906	1212	1344

Table 3
Phases detected in the XRD patterns of the LAS and YAS and Al/Si ratio in the mullite

Glass	Al/Si th.	Annealing (T °C, th)	Observed phases	Al/Si mullite	a (nm) mullite	b (nm) mullite	c (nm) mullite
LAS1	0.471	1150 °C, 15 h	$La_2Si_2O_7$				
LAS2	0.321	1080 °C, 5.30 h	Cristobalite				
LAS3	0.590	1060 °C, 2 h	Mullite	3.14	0.75459	0.76937	0.28834
LAS4	0.707	1200 °C, 2 h	Mullite + cristobalite	3.15	0.75473	0.76928	0.28839
YAS1	0.470	1100 °C, 5 h	$Y_2Si_2O_7$ + mullite	3.14	0.75459	0.76937	0.28834
YAS2	0.321	1100 °C, 5 h	$Y_2Si_2O_7$ + mullite + cristobalite	3.14	0.75459	0.76937	0.28834
YAS3	0.589	1060 °C, 2.5 h	mullite + tridymite	3.14	0.75459	0.76937	0.28834
YAS4	0.707	1200 °C, 2.30 h	$Y_2Si_2O_7$ + mullite + $Y_2Si_2O_7$* (traces)	3.14	0.75459	0.76937	0.28834

$La_2Si_2O_7$ (JCPDS-82-0729); $Y_2Si_2O_7$ (JCPDS-22-1103); $Y_2Si_2O_7$* (JCPDS-82-0732).

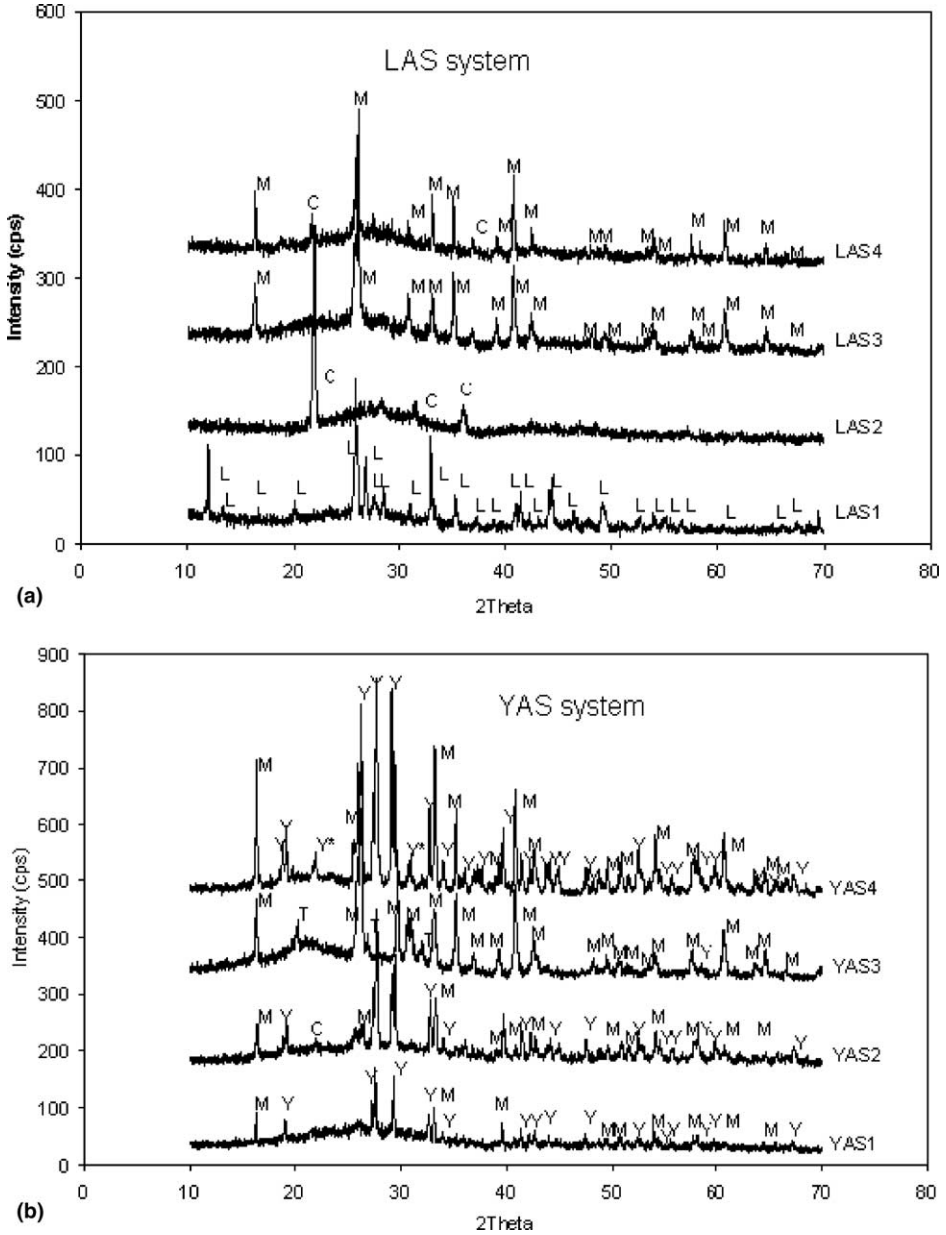

Fig. 3. X-ray diffraction patterns of annealed LAS (a) and YAS (b) glasses C = cristobalite; M = Mullite; L = $La_2Si_2O_7$; Y = y-$Y_2Si_2O_7$; Y* = β-$Y_2Si_2O_7$.

of observed micrographs are given in Fig. 4. Figs. 4(a) and (b) corresponds to long time annealing of LAS1 and LAS2 glasses (respectively 1150 °C, 15 h and 1080 °C, 5.30 h). Both exhibit the same phases: cristobalite, needle-like crystallites of $La_2Si_2O_7$ more developed in LAS1 and the residual glass. It is interesting to note that these micrographs are in excellent agreement with the X-ray data and that cristobalie crystallizes mainly at the glass/$La_2Si_2O_7$ interface in the LAS1 glass but in the bulk residual glass in LAS2. Typical micrographs of the 2 h annealing are shown in Fig. 4(c) and (d), and corresponds to LAS4 and YAS4, respectively. Residual glass analysis has been carried out by SEM-EDS. The results are given in Table 4. Results for YAS1 and YAS2 are written in italic, in these samples the size of the glassy areas is smaller than the electron beam.

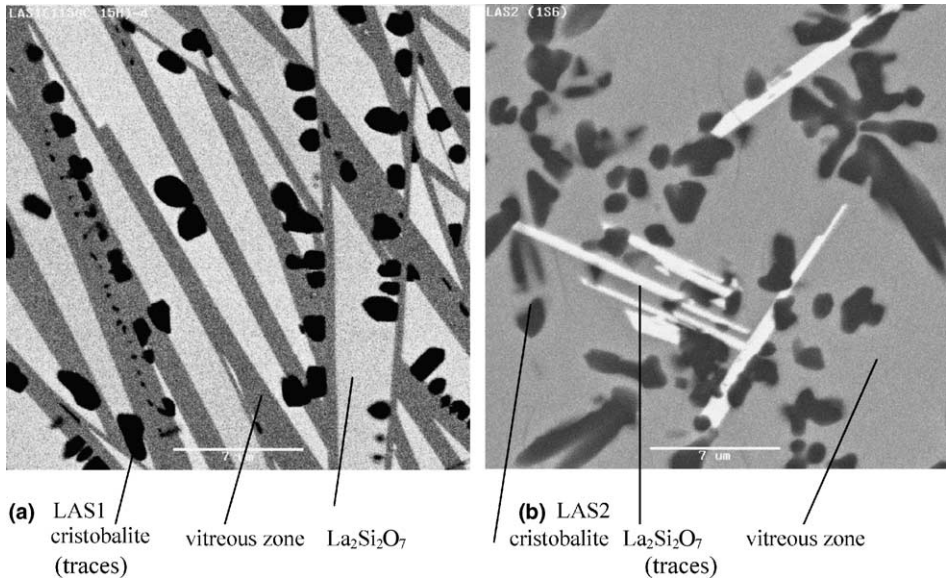

Fig. 4. SEM micrographs of LAS annealed glasses (a): LAS1 (1150 °C, 15 h), (b): LAS2 (1080 °C, 5.5 h).

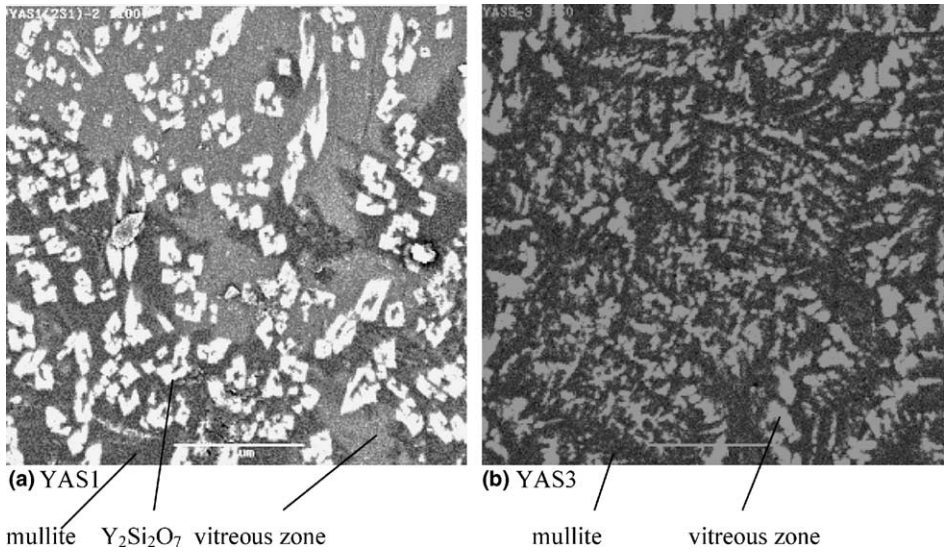

Fig. 5. SEM micrographs of YAS annealed glasses (a): YAS1 (1100 °C, 5 h), (b): YAS3 (1060 °C, 2.5 h).

4. Discussion

Our glass compositions are represented in the La_2O_3–Al_2O_3–SiO_2 and Y_2O_3–Al_2O_3–SiO_2 ternary diagrams shown in Fig. 1. In particular, the glasses YAS3 and YAS4 are out of the vitreous ranges determined by other authors [6,7]. This shows the importance of the use of a laboratory-scale solar furnace compared to the classical method with platinum metallic crucibles: (a) the interaction between the molten droplet and the surroundings is very low so that heterogeneous nucleation is minimized and (b) the cooling rate is more higher (around 200 °C s^{-1} as outlined in part 2). Concerning the evolution of the glass transition temperature, the measured T_g are higher for yttrium glasses, due to the effect of the ionic field strength (z/r^2) which even if the coordination number of the lanthanide ion is not known is greater for Y than for La. It is interesting to note that for the LAS glasses T_g increases

Table 4
Chemical compositions (atomic %) of residual glass of LAS and YAS observed after crystallization

Samples		Si	Al	Ln	O
LAS1	Parent glass	21.8	8.87	4.9	64.39
	Residual glass	16.7	10.6	3.8	68.9
LAS2	Parent glass	23.20	7.45	4.69	64.66
	Residual glass	16.7	8.8	4.5	67.7
LAS3	Parent glass	20.52	12.9	1.05	65.44
	Residual glass	18.9	15.4	1.5	63.8
LAS4	Parent glass	20.36	13.86	2.94	62.85
	Residual glass	22.3	13.5	3.8	60.0
YAS1	Parent glass	20.11	9.49	6.37	64.04
	Residual glass	*20.2*	*10.7*	*4.8*	*64.3*
YAS2	Parent glass	22.2	7.76	7.15	62.87
	Residual glass	*22.1*	*9.3*	*5.6*	*63.9*
YAS3	Parent glass	22.14	12.34	2.54	61.75
	Residual glass	20.6	10.9	3.1	65.2
YAS4	Parent glass	19.69	13.24	4.6	64.39
	Residual glass	20.1	12.8	3.5	63.6

with the Al/Si ratio while for the YAS glasses T_g seems to be independent of it. These results are in good agreement with previous results [4,8]. For example in YAS glasses, Hyatt et al. [4] have found a T_g variation between 880 and 895 °C for glasses richer in Y_2O_3 and with Al/Si ratios varying between 0.553 and 2. For the LAS glasses, the results of Aronne et al. [8] also indicate that the range of T_g is between 841 and 860 °C with Al/Si ratios ranging from 0.428 to 1.75. Concerning the effect of the Ln/Si ratio, T_g seems in a first analysis independent for YAS glasses and decreases when the La/Si ratio increases. It is clear that the effects of the glass composition on the T_g values of LAS and YAS glasses and the role of $La^{3+}/Y^{3+}$and Al^{3+} ions and the Al/Si ratio depends on several factors, in particular the detailed structure of these glasses which are not completely known.

For the YAS glasses, the differential thermal analysis results show an endothermic peak attributed to the melting of the ternary eutectic mullite–yttrium disilicate–silica with a measured temperature in very good agreement with previous experimental data [7,20] (1345–1371 °C) and recent thermodynamical assessments [19] (1349–1379 °C). The composition of this ternary eutectic in weight % is around 32% Y_2O_3, 22% Al_2O_3 and 46% SiO_2, which is very close to the YAS1 and YAS2 glass composition where the endotherms are more important than in YAS3 and YAS4.

Concerning LAS glasses, no thermal event corresponding to a melting is observed in the DTA curves up to 1550 °C.

5. Conclusion

The results obtained in this study can be summarized as follows:

1. In agreement with the literature data, as outlined previously, the glass transition temperature T_g is higher for Y glasses than for the LAS glasses. A better understanding will be available when structural studies, actually running, by solid state multinuclear NMR (^{17}O, ^{27}Al, and ^{29}Si) and X-ray and neutron diffusion will be completed.
2. In the DTA curves, melting is observed only in the YAS glasses that correspond to the ternary eutectic (composition: 32% Y_2O_3, 22% Al_2O_3 and 46% SiO_2 wt%, melting point ~1360 °C).
3. The phases observed during the crystallization of the glasses are in good agreement with the published phase diagrams and always a residual glass is observed. Concerning the residual glass, despite difficulties in accurate chemical analysis, a general trend is observed: they have always a lower silica content than the parent glasses. Due to the composition of these glasses mullite, disilicate and cristobalite are the only crystallized phases observed. For the mullite, the Al/Si ratio obtained in crystallized glasses for La and Y samples is always the same, 3.14, corresponding to a composition of the solid solution of $Al_2^{VI}[Al_{2+2x}Si_{2-2x}]^{IV}O_{10-x}$ with $x = 0.275$ very close to the value of stoichiometric 3:2 mullite ($x = 0.25$). For the disilicate, the high temperature G form is observed for $La_2Si_2O_7$ and two crystalline forms y and β for $Y_2Si_2O_7$.
4. Concerning the potential interest of these glasses for the storage of minor actinides, it is clear that crystallization is more difficult in the LAS glasses than the YAS glasses. Nevertheless, YAS1 and YAS2 glasses are close in composition to a ternary eutectic in the Y_2O_3–Al_2O_3–SiO_2 system with a melting point is around 1360 °C, an important result for manufacturing and shaping of materials including actinide oxides.

Acknowledgements

We thank CEA-Marcoule for financial support, the Région Languedoc-Roussillon for financial help

in the purchase of the DTA equipment and A. Szubarga for performing the thermal analysis measurements.

References

[1] J.T. Kohli, J.E. Shelby, Phys. Chem. Glass 32 (1991) 67.
[2] J.E. Shelby, S.M. Minton, C.E. Lord, M.R. Tuzzolo, Phys. Chem. Glass 33 (1992) 93.
[3] J.T. Kohli, R.A. Condrate, Phys. Chem. Glass 34 (1993) 81.
[4] M.J. Hyatt, D.E. Day, J. Am. Ceram. Soc. 70 (1987) C283.
[5] J.T. Kohli, J.E. Shelby, J. Am. Ceram. Soc. 74 (1991) 1031.
[6] J.E. Shelby, Key Eng. Mater., 94&95, Trans Tech Publications, Switzerland, 1994, p. 1.
[7] U. Kolitsch, H.J. Seifert, F. Aldinger, J. Phase Equilibria 19 (1998) 426.
[8] A. Aronne, S. Esposito, P. Pernice, Mater. Chem. Phys. 51 (1997) 163.
[9] A. Makishima, Y. Tamura, T. Sakaino, J. Am. Ceram. Soc. 61 (1978) 247.
[10] T. Setsuhisa, H. Kazuyuki, S. Naohiro Soga, J. Am. Ceram. Soc. 73 (1992) 503.
[11] G. Leturcq, G. Berger, T. Advocat, E. Vernaz, Chem. Geol. 160 (1999) 39.
[12] L. Bois, M.J. Guittet, N. Barré, P. Trocellier, S. Guillopé, M. Gautier, P. Verdier, Y. Laurent, J. Non-Cryst. Sol. 276 (2000) 181.
[13] L. Bois, N. Barré, M.J. Guittet, S. Guillopé, P. Trocellier, M. Gautier, P. Verdier, Y. Laurent, J. Non-Cryst. Sol. 300 (2002) 141.
[14] P. Wu, A.D. Pelton, J. Alloys Compds. 179 (1992) 259.
[15] S.S. Kim, J.Y. Park, T.H. Sanders, J. Alloys Compds. 321 (2001) 84.
[16] D. Mazza, S. Ronchetti, Mater. Res. Bul. 34 (1999) 1375.
[17] P. Vomaka, O. Babushkin, J. Eur. Ceram. Soc. 15 (1995) 921.
[18] U. Kolitsch, PhD thesis, Univ. Stuttgard, 1995.
[19] O. Fabrichnaya, H.J. Seifert, R. Weiland, T. Ludwig, F. Aldinger, A. Navrotky, Z. Metallkd. 92 (2001) 1083.
[20] N.A. Toropov, I.A. Bondar, Izv. Akad. Nauk. SSSR Otd Khim. Nauk. (1961) 547.
[21] U. Kolitsch, H.J. Seifert, T. Ludwig, F. Aldinger, J. Mater. Res. 14 (1999) 447.
[22] M. Mizuno, R. Berjoan, J.P. Coutures, M. Foex, Yogyo-Kyokai-Shi 82 (1974) 631.
[23] S. Geller, V.B. Bala, Acta Crystallogr. 9 (1956) 1019.
[24] R. Diehl, G. Brandt, Mater. Res. Bull. 10 (1975) 85.
[25] M. Gervais, S. Le Floch, J.C. Rillet, J. Coutures, J.P. Coutures, J. Am. Ceram. Soc. 75 (1992) 3166.
[26] T.S. Chernaya, Kristallografia 34 (1989) 1292.
[27] M.S. Lehmann, A. Ordlund-Christensen, H. Fjellvag, J. Appl. Crystallogr. 20 (1987) 123.
[28] N.A. Toropov, I.A. Bondar, F.I. Galakhov, K.H.S. Nicojian, I.V. Vinogradova, Izv. Akad. Nauk. SSR, Ser. Khim 7 (1964) 1158.
[29] J. Dorhup, A. Hoyvald, G. Moergensten, C.J.H. Jacobsen, J. Villadsen, J. Am. Ceram. Soc. 79 (1966) 2969.
[30] J. Dexpert-Ghys, M. Faucher, P. Caro, J. Solid State Chem. 19 (1976) 193.
[31] J. Felsche, J. Less Common Metals 21 (1970) 1.
[32] E.G. Protosenko, Zap. Vses. Mineral. Obshch. 91 (1960) 260.
[33] N.G. Batalieva, Y.A. Pyatenko, Sov. Phys. Crystallogr. 16 (1972) 786.
[34] J. Ito, H. Johnson, Amer. Miner. 5 (1968) 1940.
[35] J. Felsche, Structure Bonding 13 (1973) 100.
[36] J. Parmentier, P.B. Bodart, L. Audoin, G. Massouras, D.P. Thompson, R.K. Harris, P. Goursat, J.-L. Besson, J. Solid State Chem. 149 (2000) 16.
[37] T. Dinger, R.S. Rai, G. Thomas, J. Am. Ceram. Soc. 71 (1988) 236.
[38] B.A. Maksimov et al., Dokl. Akad. Nauk SSSR 183 (1968) 1072.
[39] V.N. Kuz'min, K.P. Belov, Dokl. Akad Nauk SSR 165 (1965) 88.
[40] N.L. Bowen, J.W. Greig, J. Am. Ceram. Soc. 7 (1924) 238.
[41] S. Aramaki, R. Roy, J. Am. Ceram. Soc. 45 (1962) 22.
[42] L.A. Aksay, J.A. Pask, J. Am. Ceram. Soc. 58 (1975) 507.
[43] (a) F.J. Klug, S. Prochazka, J. Am. Ceram. Soc. 70 (1987) 750;
(b) F.J. Klug, S. Prochazka, in: S. Somiya, F. Davis, J.A. Pask (Eds.), Ceram. Trans., vol. 6, The American Ceramic Society, Westerville OH., 1990, p. 1.
[44] G. Eriksson, A.D. Pelton, Metal. Trans. B 24B (1993) 807.
[45] Thèse I Jaymes, Thèse de Doctorat, Université d'Orléans, 1995.
[46] Natl. Bur. Stand. (U.S) Monogr. 25 (1964) 3.
[47] W.E. Cameron, Am. Mineral. 62 (1977) 47.
[48] T. Ban, K. Okada, J. Am. Ceram. Soc. 75 (1992) 227.